Journal of Medicinal and Nanomaterials Chemistry 1 (2022) 63-78

Journal of Medicinal and Nanomaterials Chemistry

Journal homepage: https://jmnc.samipubco.com/

Original Research Article

The investigation of antibacterial activity and cell viability of rGO/Cu_2O nanocomposite

Ali Oji Moghanlou*, Farshid Salimi

Department of Chemistry, Ardabil Branch, Islamic Azad University, Ardabil, Iran

ARTICLE INFORMATION

Received: 25 December 2021
Received in revised: 29 January 2022
Accepted: 2 February 2022
Available online: 11 February 2022

DOI: 10.48309/JMNC.2022.1.6

KEYWORDS

rGO/Cu_2O
Nanocomposite
Photocatalytic properties
Antibacterial activity
Toxicity

ABSTRACT

With pathogenic microorganisms such as bacteria around our lives, research and finding an effective antibacterial agent is essential. This study prepared and developed a novel nanocomposite based on photocatalytic properties. For grafting of copper (I) oxide nanoparticles in reduced graphene oxide sheets, the simultaneous reduction reaction of graphene oxide and copper (II) acetate monohydrate salt in the presence of sodium borohydride was used to reduce agent. Fourier transform infrared spectroscopy (FTIR), X-ray photoelectron (XPS), X-ray diffraction (XRD), field emission scanning electron microscopy (FESEM), Transmission electron microscopy (TEM), Energy-dispersive X-ray (EDAX), and Raman spectroscopy studied and identified the prepared nanocomposite. These studies showed that 2D rGO is well-decorated by Cu_2O nanoparticles. The results of antibacterial tests showed that the synthesized nanocomposite has excellent antibacterial properties, and due to exposure to UV light for 6 h, these properties have been increased. Also, the toxicity of nanocomposite indicated that this agent had biocompatibility properties.

Corresponding author, email: ali.oji1972@yahoo.com (A. Oji Moghanlou).

Graphical Abstract

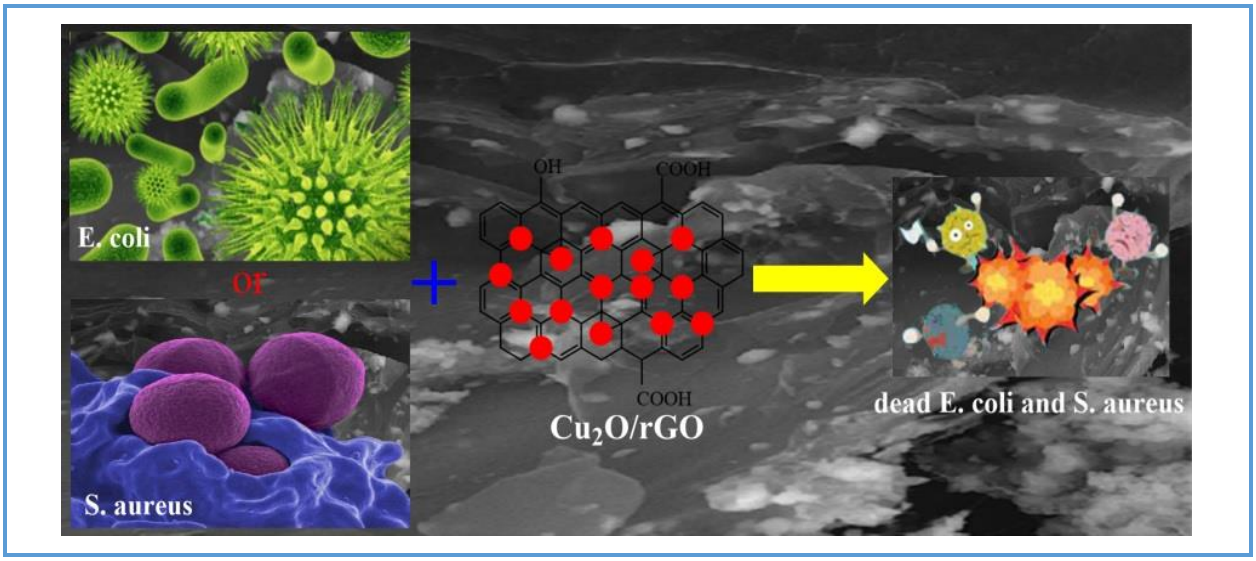

Introduction

Graphene and its derivatives are known as an antibacterial substrate, and it is expected to be used in the future for antibacterial coatings [1]. Graphene oxide (GO), one of the derivatives of graphene, is the product of the oxidation of graphene. It has attracted a lot of attention due to its suitable hydrophilicity and surface functionalization ability due to abundant oxygen in functional groups [2]. GO can be converted to reduced graphene oxide (rGO) by thermal annealing or chemical reduction methods, during which the functional groups are primarily eliminated [3].

High surface area, good thermal stability, and high conductivity are the characteristics of rGO sheets. rGO also has many applications in various fields such as electronics, electrochemistry, sensors, photodetectors, transparent conductors, batteries, detectors, and catalysts to reduce toxic organic compounds [4–11]. However, the use of rGO products in medicine and food technology makes it difficult for its weak antibacterial abilities [12–14]. For that reason, the preparation of antibacterial rGO products seems to be of high importance. Numerous studies have reported these two types of GO-based substances (GO and rGO) [15, 16].

The synthesis of Ag/rGO was reported in 2014. Ag/rGO was prepared in this research by reducing silver nitrate on GO layers synthesized from graphite powder. In this synthesis, the conversion of graphite to GO is complicated and involves complex steps [17, 18]. Therefore, large-scale synthesis of Ag/rGO is impossible and very difficult. Abolfazl Bezaatpour *et al*. reported the synthesis of rGO/$BiVO_4$ in 2019. This research involves simultaneous reduction reaction of GO and bismuth nitrate by hydrothermal method. In this paper, the preparation of new heterogeneous $BiVO_4$/rGO nanocomposites based on rGO and bismuth vanadate ($BiVO_4$) was reported [19]. Rabah Boukherroub synthesized rGO/NiO recently. To prepare rGO/NiO nanocomposites, nickel oxide nanoparticles were bonded to the rGO is a single-step reaction with simultaneous reduction of GO and $NiCl_2$ [20]. In 2019, Turpu *et al*. prepared rGO/$FeVO_4$ nanocomposites from the reaction of $Fe(NO_3)_3$,$9H_2O$ and NH_4VO_3 in nitric acid solution using hydrothermal method [21].

Antibacterial activity of rGO/TiO_2 nanocomposite against Enterobacter hormaechei was reported by Yanbin Xu et al. They showed that rGO coupled with TiO_2 nanoparticles increased antibacterial activity against Enterobacter hormaechei under visible and UV light compared to rGO or TiO_2 alone [22]. Facile preparation of Fe_3O_4/Ag/RGO was reported by Hongri Wan et al. They used the hydrothermal method to prepare tri-recyclable Fe_3O_4/Ag/RGO nanocomposites. Also, they investigated the catalytic activity and antibacterial effect of their nanocomposites [23]. PEG/MoS_2/rGO nanoparticles were prepared using the hydrothermal method by Hualin Wang *et al*. Their cytotoxicity and antibacterial effect against Staphylococcus were investigated [24]. The literature reported the synthesis of rGO/ZnONR nanocomposites by coupling zinc oxide nanorods (NR) on rGO [25]. These nanocomposites could produce hydrogen under sunlight and had antibacterial and photocatalytic properties. They revealed excellent performance in the effective decolorization of textile dyes and controlling E. coli and S. aureus bacteria.

Cu_2O nanoparticles are one of the best materials for environmental applications, even in low concentrations. They are environmentally friendly, non-toxic, inexpensive, and abundant [26, 27]. Cu_2O nanoparticles and other copper compounds have various applications such as gas measurement, antifungal, anti-algae, antibacterial, photocatalytic, photocatalytic destroyer of environmental pollutants and wastewater, anti-fouling, in water and wastewater treatment, dye, pharmaceutical, and organic degradation as well used in solar cell technology [28–34]. Some studies show that copper compounds have strong antibacterial effects. For example, copper (II) sulfate enhances the antibacterial activity of silk fiber [35]. Cu_2O, in comparison with CuO, has a higher antibacterial effect. Also, Cu_2O is used as an antibacterial agent [36, 37] and fungicide [38, 39]. In some cases, Cu_2O shows higher lethality than Ag [40].

However, the study of antibacterial properties and toxicity of rGO/Cu_2O nanocomposites has not been widely considered. We reported identifying and investigating the photocatalytic properties of rGO/Cu_2O nanocomposite to reduce harmful and toxic nitroaromatics to beneficial amino aromatics [41]. This research investigates the antibacterial activity and toxicity of the aforementioned nanocomposite based on its photocatalytic properties. Attempts have been made to synthesize this nanocomposite with conventional methods and using the least chemicals with low toxicity. Unlike similar works, this research focused on nanocomposites' photocatalytic properties, which can achieve the highest antibacterial properties.

Experimental

Materials and methods

The required chemicals were purchased from Fluca and Merck and used without refining.

Preparation of graphene oxide (GO)

Graphene oxide was prepared, with some variations, based on modified Hummers' method [41].

Preparation of rGO/Cu_2O nanocomposite

For the preparation of rGO/Cu_2O nanocomposite, the simultaneous reduction reaction of graphene oxide and copper (II) acetate monohydrate salt in the presence of sodium borohydride was used [41].

Chemical characterization of rGO/Cu_2O

The prepared nanocomposite was studied and identified by Fourier transform infrared spectroscopy (FTIR), X-ray photoelectron (XPS), X-ray diffraction (XRD), field emission scanning electron microscopy (FESEM), transmission electron microscopy (TEM), energy-dispersive X-ray (EDAX), and Raman spectroscopy [41].

To study biological behavior, Samples are selected, including Cu_2O, GO, rGO, and X as nanocomposites of rGO/Cu_2O, and to investigate the effect of photocatalysis, nanocomposites are treated with visible light for 6 h (X1), a UV light for 3 h (X2) and UV light for 6 h (X3).

Biological activities

Assessment of antibacterial activity

An approach, agar well diffusion, containing agar and other materials, was utilized to identify the antibacterial activity of the prepared nanocomposites of copper and graphene (Cu_2O, GO, rGO, and Cu_2O/rGO). The applied approach was versus *Escherichia coli* (ATCC 25922) and *Staphylococcus aureus* (ATCC 25923). In this approach, the bacteria were flourished on Mueller Hinton Broth (MHB) medium. Then suitable procedures relating to the approach were done at 37 °C for 18 h. Later on, the cultivation media were developed by punching. For a reasonable comparison, a volume of 60 µL of the equivalent concentration of each chemical was then added to each well. After that, the incubation condition of 37 °C for 18 h was exerted to the plates. A standard ruler was utilized to measure the diameter (in mm) of the inhibition region. The Minimum Inhibitory Concentration (MIC) was determined using a two-fold serial dilution method (Subcommittee on Antifungal Susceptibility Testing (AFST) of European Society of Clinical Microbiology and Infectious Diseases (ESCMID), European Committee for Antimicrobial Susceptibility Testing (EUCAST). The growth of inoculum (test organisms) was adjusted to 1% McFarland standard. 13 g of nutrient broth was diluted to 1000 mL by distilled water. In this way, the nutrient broth was prepared. Then, it was autoclaved at 121 °C, for 15 min. A 96 well microtiter plate was used for broth dilution. 100 µL of the diluted conidial inoculum suspensions (two times) was added to each well in the plate. With this addition, the final volume in each well reached 200 µL. The rGO/Cu_2O nanocomposite was diluted in DMSO to a final concentration of 10 mg/mL and the following amounts (in mg) were developed, 0.0625, 0.125, 0.250, 0.5, 1.0. All of them were incubated at room temperature overnight. We had a control well containing only organisms. Using visual inspection, growth in the samples was observed. An ELISA plate reader estimated the growth by absorbance (Abs.) values at 630 nm. The percentage of inhibition in the antimicrobial test for all of the wells was calculated as follows:

$$\text{Percentage of Inhibition} = \frac{\text{Abs. of control} - \text{Abs. of the test}}{\text{Abs. of control}} \times 100$$

Two essential factors for measuring antibacterial activity are minimum inhibitory concentration (MIC) and minimum bacterial concentration (MBC). MIC is the minimum concentration at which no colony occurred. MBC is a symbol for a case where the number of bacteria is less than 10. The whole of devices (e.g., graduated cylinders, pipette tips, culture dishes, media, deionized water, PBS solution, etc.) were sterilized in the autoclave before

experiments. All of the experiments were done in the sterilized situation. Elimination of experimental errors is necessary, so tests of this step were carried out with three parallel experiments. In this method, tetracycline antibiotic was used as a positive control. Also, due to the use of PBS solvent, due to the lack of antibacterial properties, there was no need to use a negative control.

Cytotoxicity assay

The cytotoxicity of synthesized nanocomposites was investigated by MTT colorimetric procedure. Briefly, MCF-7 cells were seeded in 96 well plates at the density of 5000 cells/well in the presence of 100 µL cell culture medium (DMEM supplemented with 10% FBS and 1% penicillin-streptomycin solution). The incubation of cells was carried out in a medium containing 5% CO_2 at 37 °C for 24 h. After this period, the same media was substituted with fresh media together with diverse concentrations of ingredients. Then the system was incubated at 37 °C for 24–72 h. The cell viability was studied by replacing the cell-containing media with a pure medium with a volume of 100 µL. Afterward, 10 µL of MTT solution (5 mg/mL in DMSO) was poured to each well and the incubation was continued for another 4 h. Then The MTT solution was discarded, after that, 100 µL of DMSO was added to each well, and they were incubated in the absence of light for 40 min. Afterward, the absorbance of the solutions was recorded at 492 nm using a microplate reader (Bio-Rad, USA).

Results and Discussion

Synthesis and characterization of rGO/Cu_2O

The simultaneous reduction reaction of GO and copper (II) acetate monohydrate in the presence of sodium borohydride was used for the synthesis of rGO/Cu_2O nanocomposite [41]. FTIR was utilized to identify functional groups in GO and rGO (Figure 1**a**). X-ray diffraction (XRD) was employed to determine the crystalline structure of the synthesized rGO and GO (Figure 1**b**). The above methods confirmed the decoration of nanoparticles on the surface of reduced GO sheets. The morphology and dimension of the nanoparticles were determined by field emission scanning electron microscopy (FESEM) (Figure 1**c**) and transmission electron microscopy (TEM) (Figure 1**d**). Owing to the intrinsic direct bandgap nature, p-type attributes, robust electrochemical behavior, and the low cost for fabrication, the studies over CuO nanomaterials have a drastic rise in a wide variety of fields [42, 43]. Cu_2O and CuO are two widespread forms of copper oxide polymorphism found in nature. One can find these materials as stoichiometric compounds in the entire CuO systems [44].

Evaluation of antibacterial properties

The antibacterial activity of the synthesized nanocomposites was measured by the disk diffusion method using Gram-negative *E. coli* and Gram-positive *S. aureus* bacteria in various exposure situations under the light of inhibition regions and measuring absorbance values at 600 nm during their interactions. The numerical value of the inhibition diameter and different samples' areas are illustrated in Figures 2 and 3, respectively.

From Figures 2 and 3, it can be concluded that compared with the GO samples, the rGO, Cu_2O, and rGO/Cu_2O nanocomposites showed a toxic effect on bacteria. It was noticed that the antibacterial activity of the lighted nanocomposite with visible light (X1) is similar to the untreated nanocomposite (X).

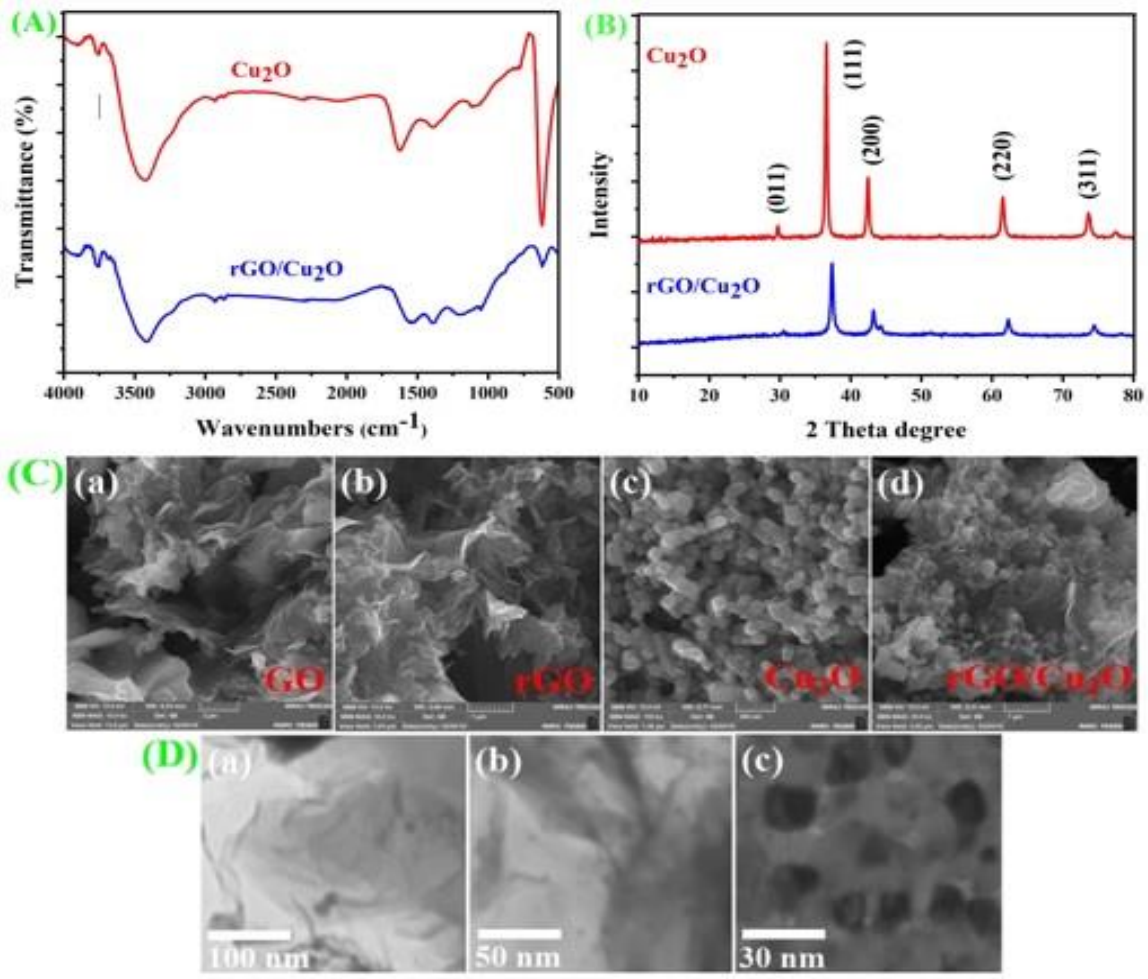

Figure 1. Characterization of nanocomposite FT-IR spectra of a) Cu_2O and rGO/Cu_2O, XRD pattern of b) Cu_2O and rGO/Cu_2O, FESEM images of a) GO, b) rGO, c) Cu_2O and d) rGO/Cu_2O, and TEM images of a-c) rGO/Cu_2O

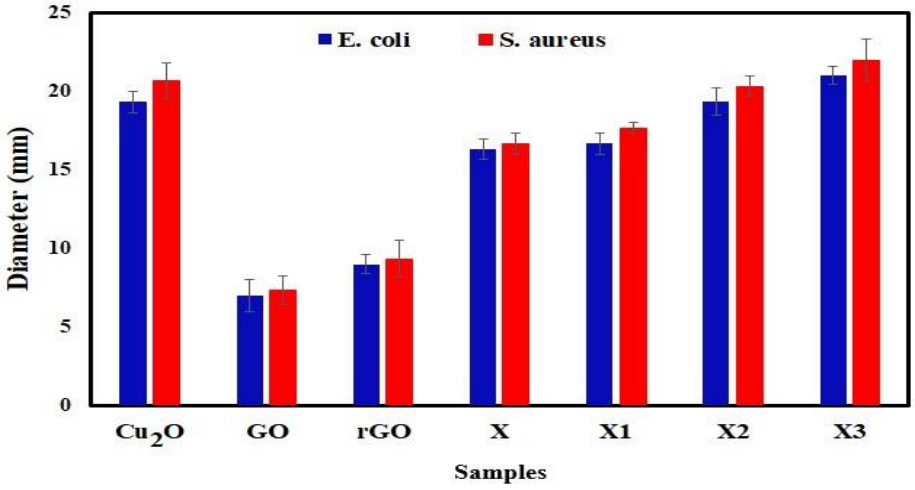

Figure 2. Diameter of zone inhibition for treated different samples with bacteria

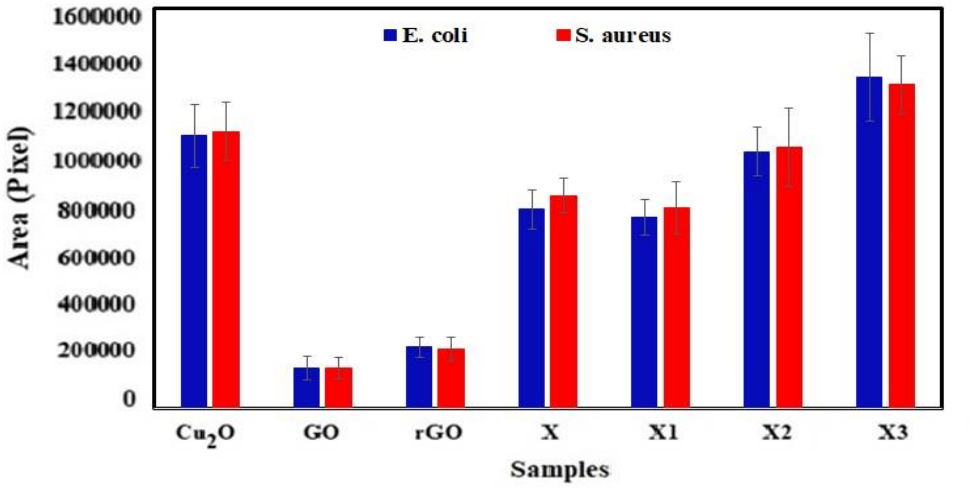

Figure 3. Area of zone inhibition for treated different samples with bacteria

However, the antibacterial properties of the treated sample with UV for 6 h were increased significantly. It indicates photocatalytic properties of nanocomposite with UV for 3 h and 6 h. The images of zone inhibition (ZI) of bacteria growth for the different samples have been shown in Figure 4. The rGO/Cu_2O nanocomposite showed a more significant zone inhibition compared to other samples, which is illustrated with the synergistic antibacterial activity of the nano-system.

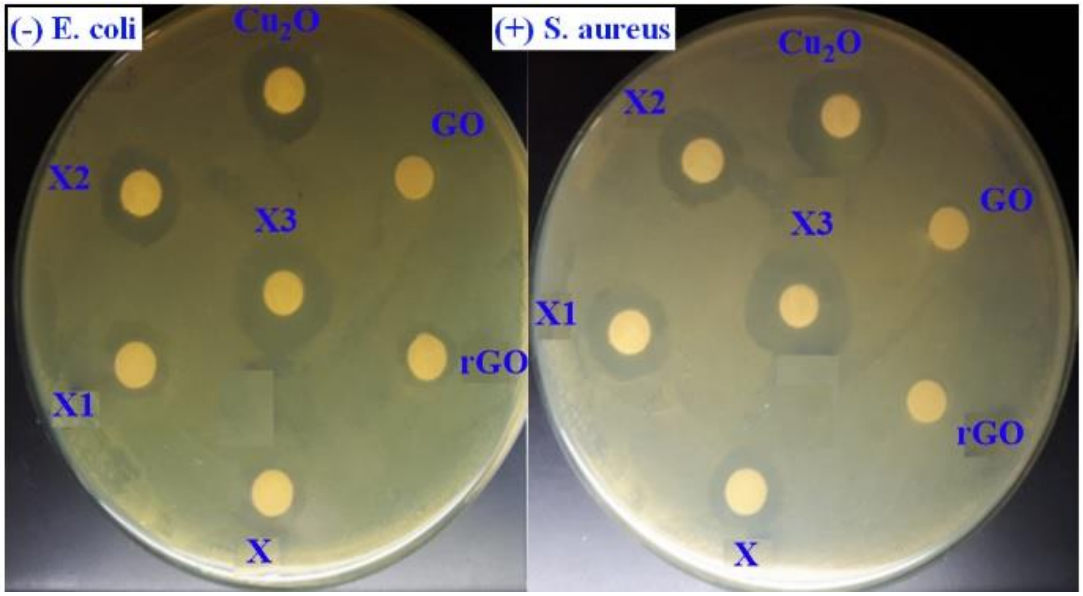

Figure 4. The image of zone inhibition of bacterial growth

Figures 5 and 6 show the percentage of *S. aureus* and *E. coli* colonies incubated with different samples. The bar charts display that the samples of GO and rGO have a lower bacterial reduction in comparison with the Cu_2O and nanocomposites. It is found that GO and its derivatives have little antibacterial activity.

Bacterial illness composes a hard difficulty in different aspects of everyday life. It causes pain in various parts of the body, and in some cases, it leads to death. Consequently, it produces unexpected enormous costs for protecting against bacterial diseases worldwide. Also, they affect other industries, namely biomedicine, food packaging, and cloth. Although academics and researchers have fulfilled comprehensive attempts in this field, there are no absolute and general solutions to confine bacterial growth. Antibacterial nanomaterials have inherent or chemically incorporated antibacterial activity and high specific surface area, so their use is a promising approach to attack against the bacteria. Graphene, GO, rGO possesses excellent electrical, thermal, and mechanical properties. They are both ultra-thin biocompatible nanomaterials and an appropriate nomination for confining bacterial infections. Diverse mechanisms are present for describing the antimicrobial function of graphenes in the literature [45–47], for instance the development of reactive oxygen species (ROS), destruction of bacteria, and the escaping of some compounds from the cell. Also, the pointed edges of graphene damage the cell. Besides, thermal and mechanical movements are other factors influencing cell disintegration. Three remarkable steps describing the antimicrobial function are: (i) adsorption of the cell on the surface of graphene, (ii) the effect of the pointed edges of graphene on the cell, (iii) oxidation by superoxide anion. Graphene nanomaterials have antimicrobial characteristics. They can form conglomerates and have strong van der Waals interactions among their sheets. Although they possess the mentioned properties, changing their surfaces by metal oxides or ions can prohibit them. The amplification of their properties is carried out by inorganic nanoparticles. Novel properties emerge in the modified nanoparticles, for instance electro-optical properties etc. Their dispersibility in water as a polar solvent is enhanced when the mixture of graphene, rGO, and metal oxide is utilized [48]. These researches show that rGO thin films are well-decorated by Cu_2O nanoparticles. Antibacterial outcome illustrated that the synthesized nanocomposite showed the highest antimicrobial properties. The discrepancy in antimicrobial effect between rGO/Cu_2O nanocomposites and Cu_2O nanoparticles was chiefly assigned to the copper ion liberate characteristics and dispersibility. The rGO/Cu_2O nanocomposite still keeps a noticeable copper ions sterilization effect by arresting the liberation of copper ions and decreasing the mass loss of Cu_2O [49]. In addition, the dispersibility of Cu_2O nanoparticles had been improved after linking Cu_2O and rGO that owned significant solubility by electrostatic interactions, consequently increasing the tangible area with bacteria. The improved antimicrobial mechanisms of rGO/Cu_2O nanocomposites resulted from the synergistic effect of constant liberation of copper ions. This effect raised ROS formation capability and great dispersal of rGO/Cu_2O nanocomposites. The in vivo production of ROS leads to the oxidation of the functional proteins and the DNA. These reactions consume reducing agents such as NADPH and cause weakened metabolic activities [50]. It is useful to claim that the antibacterial activity of nanoparticles is based on based on not only their physicochemical properties but also the biological characteristics of target microorganisms. This study agrees with others' results, indicating that the Gram-positive strains displayed greater resistance against nanoparticles when compared with Gram-negative ones [51–53]. Cu (I) species that is accommodated in the internal part of rGO are considered the most responsible factor of the

intense antimicrobial property of rGO/Cu_2O because the mentioned species have bactericidal property. Although Cu (I) species have low cost, they exhibit surpassing antimicrobial characteristics compared to many other noble metals. It was supplied an adequately stable place for the Cu_2O nanocrystals by rGO. This situation prohibited Cu_2O nanocrystals from accumulation into bulk form, and consequently, rGO protected noticeably antimicrobial capability of the Cu (I) nanocrystals. Considering all of the mentioned points, one can deduce that small amounts of Cu_2O in the structure of rGO improve its antimicrobial activity remarkably. Due to the powerful susceptibility of electron donation by Cu (I), reports indicated that Cu (I) exhibits excellent antimicrobial activity relative to other cupric species [54]. Protein denaturation due to Cu (I) contact is considered a mechanism of cytotoxicity. In addition, the production of ROS compounds leads to damaging cellular components. Therefore, the mentioned results showed severe antibacterial activity of low-cost rGO/Cu_2O nanocomposite. Nanoparticles have been shown to have an excellent antimicrobial property compared to their bulk counterparts because they possess a higher surface-to-volume ratio. This property increases the contact area with bacteria. Model microorganisms, i.e., *E. coli* and *S. aureus* have been usually utilized when the antibacterial characteristics of nanomaterials have been studied. In connection with this, developing investigations must be concentrated on other bacteria such as S. *Epidermidis, S. enteritidis, S. typhimurium P. aeruginosa, E. faecalis, and B. subtilis*. These studies help us have widespread attitudes about the antimicrobial capability of graphene-based nanomaterials. These boost antibiotic resistance among various bacteria and their association as a critical menace to human health worldwide. Generally, these nanomaterials give rise to the more intensive detriment to *E. coli* than Staphylococcus aureus because of structural dissimilarities and the biochemical composition of the cellular membrane. Gram-positive bacteria have one cytoplasmic membrane and a dense wall consisting of multilayers of peptidoglycan. On the other hand, Gram-negative bacteria possess a multipart cell wall structure, with a peptidoglycan layer between the outer membrane and the cytoplasmic membrane. Nevertheless, discrepancies in nanomaterial concentrations, production routes, antibacterial measurement methods, etc., make the comparison of antibacterial activities to be hard. Other factors such as shape, size, defects, and functional groups of surfaces affect the antimicrobial activities. Aggregated nanomaterials exhibit weaker antimicrobial properties than the well-dispersed ones. In addition, when the size of nanoparticles is small, they act more efficiently because they expose a larger surface of themselves to bacteria. On the contrary, if the nanoparticle has a triangular shape, it will reveal more effective activity than spherical ones against Gram-positive and Gram-negative bacteria. When a nanoparticle has sharp edges, its penetration power to the cellular membrane will be high, and its entrance to the cell membrane will be easy. There are combinations of various mechanisms that control the antimicrobial activity of a given nanocomposite. Some of them are as below; entrance through the cellular membrane, the liberation of inorganic nanoparticle ions, DNA, ROS production, mitochondrion, protein, lipid damage, and interruption of a bacterial cell. It seems that the last mechanism plays a key role versus Gram-negative bacteria. On the other hand, the DNA, mitochondrion, protein, and lipid damage seen when a cell is prohibited during division account for the disintegration of Gram-positive ones. Although the survey about

the antibacterial mechanism of nanomaterials containing graphene has been done in recent years, there are many unknown issues in this field and many debatable data are present in different reports. Thus, many investigations about their mechanism are required so that our knowledge becomes comprehensive and deeper. The high priority duty of researchers is achieving the true mechanism of bacteria and graphene-based nanomaterials. Also, the influence of various factors such as oxygen content, lateral size, basal planes, etc., is debatable in this field. Additional confrontation is toxicity testing of graphene containing nanomaterials. Despite several investigations on this topic, there are disagreements among the results and problems about universal acceptance criteria for the toxicity of these nanomaterials. This problem must be solved before its applications in alive biological systems. Despite challenges, it seems that remarkable progresses will be revealed about these antimicrobial nanocomposites in the future. Overall, rGO/Cu_2O nanocomposite faced an effectively greater colony reduction rate than with the other samples, specificity exposed nanocomposites with UV have a considerable influence on antibacterial reduction. It is noticeable that it is no difference between antibacterial activity in the lower concentration of samples, including 0.125 and 0.25 mg/mL, so based on the results, the optimum concentration for maximum antibacterial activity was determined 1 mg/mL. Furthermore, all nanocomposites can reduce Gram-positive S. aureus more than Gram-negative E. coli bacteria, which may be due to a greater plasma layer of Gram-negative bacteria than Gram-positive bacteria. The results of MIC and MBC are shown in Table 1. The antibacterial activities of the synthesized nanomaterials were studied using the determination of the viability of each bacterial strain based on its absorbance at 600 nm (Abs_{600}). Further, the obtained results were not only in agreement with MIC and MBC results, but they also revealed that the nanoparticles can lessen microbial viability at concentrations less than MIC. The results show that Cu_2O and treated nanocomposite by UV for 6 h are the best antibacterial agent for inhibiting the bacteria growth. However, Cu_2O with a 5 mg/mL concentration is the most effective against *S. aureus*. GO and its derivatives with high engagement can inhibit the bacteria growth and X, X1 and X2. However, the results of MBC presented in Table1 indicate that the highest rate of antimicrobial activity for destroying the bacteria is related to Cu_2O with the lowest concentration (2.5 mg/mL). In comparison, nanocomposite treated with UV for 6 h with a higher concentration (5 mg/mL) than Cu_2O has bactericidal properties. Overall, it is found that the nanocomposite shows the photocatalysis activity that inhibits the bacteria growth. Although the true mechanism of nanomaterials-mediated antimicrobial activity has not been adequately introduced, diverse conceivable routes were recommended in the literature considering the antimicrobial activity of nanomaterials [55]. The linking capability of the nanomaterial causes its penetration into the cellular membrane. Therefore, the bacterial membrane is changed. Consequently, the bacterial membrane's structural integrity loses and leads to bactericidal activity of the bacterial cells [55].

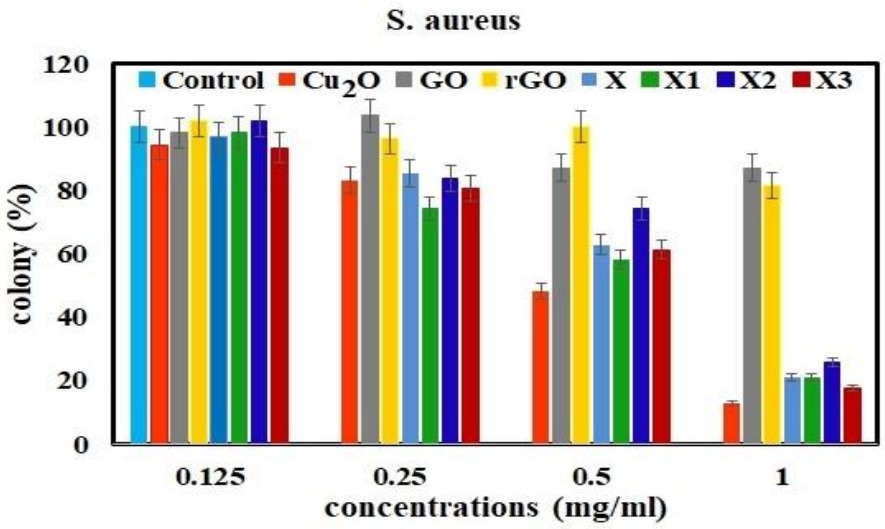

Figure 5. Antibacterial activity of selected samples with different concentration using Pour Plate method (*S. aureus*)

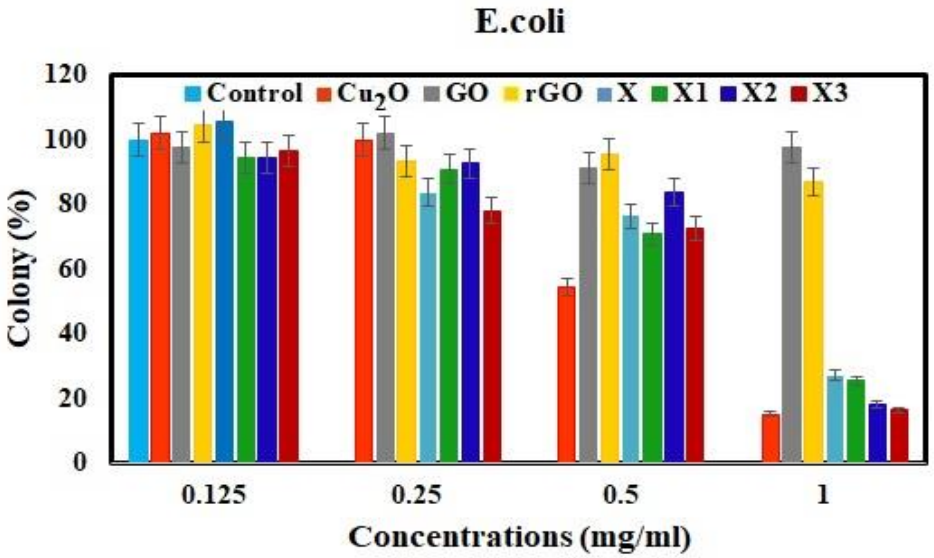

Figure 6. Antibacterial activity of selected samples with different concentrations using Pour Plate method (*E. coli*)

Table 1. The MIC and MBC of selected samples

	MIC (mg/mL)						
	Cu_2O	GO	rCO	X	X1	X2	X3
E. coli	5	-	20	10	20	10	5
S. aureus	2.5	20	10	10	10	5	5
	MBC (mg/mL)						
	Cu_2O	GO	rCO	X	X1	X2	X3
E. coli	2.5	-	-	-	-	-	5
S. aureus	2.5	-	-	-	20	10	10

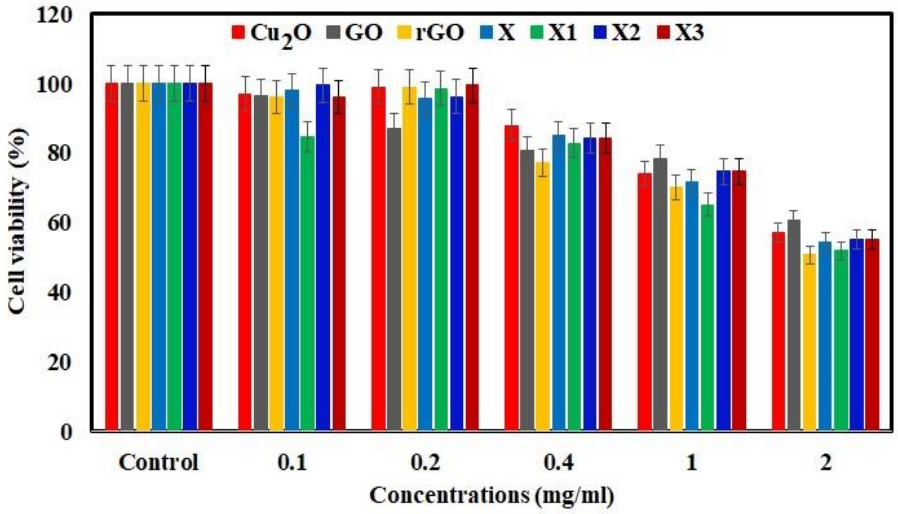

Figure 7. The cell viability of samples with cells

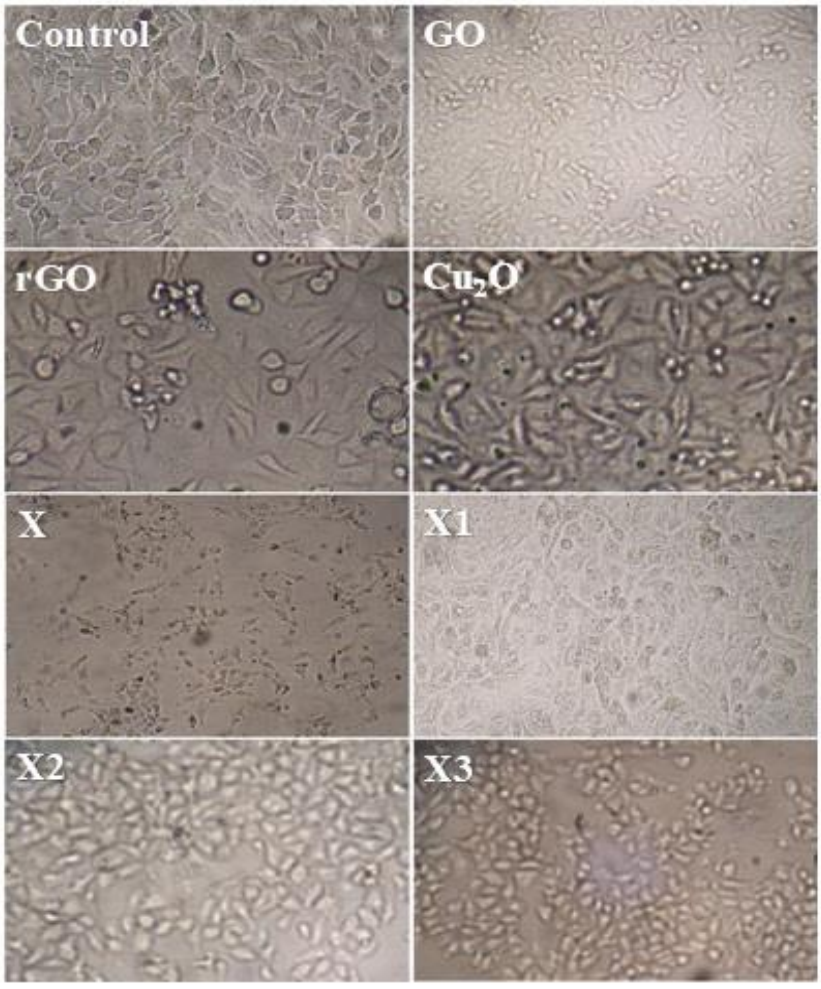

Figure 8. The images of treated cell with selected samples

Cytotoxicity analysis

The cytotoxicity of the prepared nanocomposites was investigated versus MCF-7 tumor cells in the period of 72 h by MTT colorimetric assay. Figure 7 illustrates the number of alive cells (based on the percentage of the control sample) after different samples incubated fibroblasts. As Figure 8 shows, rGO/Cu_2O nanocomposites exhibit higher levels of cytotoxicity, whereas they are a reduced form of GO, since they reduced the viability of cells by 80%. As can be seen, by increasing the concentrations of samples, the cell viabilities of all samples are decreased, so particles and the nanocomposite with the highest concentration have cell toxicity. The optimum concentration for all samples with appropriate cell viability is 0.2 and 0.4 mg/mL. Based on the antibacterial results, 0.4 mg/mL is the optimum concentration for both goals. It is found that nanocomposite exposure to UV for 6 h and goes have high cell viability than other samples. Again, there is lower antibacterial properties for GO, X3, so they were selected as good samples with photocatalysis activity. Despite the significant reduction in the cells' survival, the images of treated cells by different samples (Figure 8) show that the morphology of cells has not changed considerably.

To sum up, the nanocomposite rGO/Cu_2O regarding UV exposure has a combination of antibacterial activity and biocompatibility. With increasing the concentration of nanocomposite and other particles, toxicity is increased. It seems that introducing the rGO/Cu_2O nanocomposites in the cell medium some of the important essential organelles such as mitochondria were targeted extremely. The reason is that some reactive radicals such as O^-, O_2^- are formed. Consequently, a disability appears in the vital metabolism of the cells, and their lives come to an end [56]. Compulsory oxidation which ROS produces is related to the activation of the caspase pathway. Various cellular reactions are arisen by the activation of caspase-3. These are proliferation, differentiation, survival, and death. Castiglioni's research group claimed that cytotoxicity is not prohibited by antioxidants in some cells (T24 cells). Subsequently, there are other mechanisms for cell toxicity in various cells [57]. Nanoparticles of Copper oxide are two types, CuO and Cu_2O. In some investigations, it has been reported that CuO toxicity is related to ROS production and lipid peroxidation. At the same time, the report has claimed that Cu_2O can damage DNA [58]. Therefore the toxicity of Cu_2O nanoparticles must be studied because it is said that water is the source of this species [59]. Also, the solubility of nanoparticles is a real threat for the environment and their effects on ecosystems [60]. Some investigations believe that the unusual stability of the nanoparticles is the origin of their penetration, accumulation, and their large quantities in the body of living things [60]. However, it is not apparent how much of the toxicity of nanoparticles is related to released metal. It seems that the break of the cellular membrane is the reason for the toxicity of nanoparticles containing copper [61]. Since the concentration of O_2 in the cellular membrane is higher than the inside part of the cell, Cu nanoparticles can be oxidized during entrance the cellular membrane. As a result, Cu ions are produced. So, the destruction of the cell occurs during metal liberation into the cell. After this step, in situ production of hydrogen peroxide at the cellular membrane happens [62]. The destruction of the cellular membrane is caused by (i) copper ion liberation into the cell (ii) direct interaction of human alveolar epithelial cell line A549 to copper ions. The later causes less toxic damage [60, 63]. Note that the copper ion liberation from Cu nanoparticles into the neighborhood of the outer part of the

membrane is a crucial step in nanoparticles of Cu toxicity. In alternative investigations, nanoparticles of Cu covered by carbon and $CuCl_2$ have been utilized. In both cases, the cellular membrane was not ruptured. However, nanoparticles of Cu damaged the cellular membrane [64]. It seems that at the end of penetration of Cu nanoparticles into the cell, they are degraded and converted to Cu^{2+} ions. Therefore, at first, the nanoparticles of Cu bring toxicity to the cancer cells. Then, they liberate Cu^{2+} ions. Cu^{2+} ions have no cytotoxic property under the concentration of 500 μM.

Conclusions

The synthesized nanomaterials displayed formidable antibacterial and cytotoxic properties while being used in-vitro, which formed a part of the curative property of the nanomaterials. The antimicrobial property of the prepared nanoparticles results from various mechanisms, including the liberation of inorganic nanoparticle ions, the entrance of nanoparticles into the cellular membrane, the emergence of ROS, DNA, protein, mitochondrion, and lipid disintegration and the break up of bacterial cell. Later is responsible for Gram-negative bacteria destroying DNA, protein, mitochondrion, and lipid that results in prohibiting cell cleavage explains the disintegration of Gram-positive bacterial ones. The results of this study revealed that the exposure of the nanocomposite to UV light is caused the bactericidal power is increased. Also, its photocatalytic properties raised this feature; this increase was introduced to produce the most antibacterial properties with the lowest concentration of the substance. Based on the results of this study, exposure to visible light did not affect antibacterial properties. Thus, the mentioned approach could be considered a suitable method for preparing this nanocomposite. Using this method, one would synthesize excellent antibacterial material with significant biocompatibility.

Acknowledgments

The authors would like to appreciate the spiritual support of the Islamic Azad University, Ardabil Branch, and especially the laboratories of the Department of Chemistry.

Disclosure Statement

No potential conflict of interest was reported by the authors.

Orcid

Ali Oji Moghanlou 0000-0001-6134-485X

Farshid Salimi 0000-0003-1379-8720

References

[1]. Han W., Wu Z., Li Y., Wang Y. *Chemical Engineering Journal,* 2019, **358**:1022

[2]. Zhu Y., Murali S., Cai W., Li X., Suk J. W., Potts J.R., Ruoff R.S. *Advanced Materials,* 2010, **22**:3906

[3]. Luo D., Zhang G., Liu J., Sun X. *The Journal of Physical Chemistry C,* 2011, **115**:11327

[4]. Moghanlou A.O., Sadr M.H., Bezaatpour A., Salimi F., Yosefi M. *Molecular Catalysis,* 2021, **516**:111997

[5]. Chitara B., Krupanidhi S., Rao C. *Applied Physics Letters,* 2011, **99**:113114

[6]. Ji L., Zhou W., Chabot V., Yu A., Xiao X. *ACS Applied Materials & Interfaces.,* 2015, **7**:24895

[7]. Bae S., Kim S.J., Shin D., Ahn J.H., Hong B.H. *Physica Scripta.,* 2012, **2012**:014024

[8]. Russo P.A., Donato N., Leonardi S.G., Baek S., Conte D.E., Neri G., Pinna N. *Angewandte Chemie International Edition,* 2012, **51**:11053

[9]. Becerril H., Mao J., Liu Z., Stoltenberg R., Bao Z., Chen Y. *ACS Nano* 2008, **2**:463

[10]. Zhang J., Liu J., Peng Q., Wang X., Li Y. *Chemistry of Materials,* 2006, **18**:867

[11]. Zhu H., Wang J., Xu G. *Crystal Growth and Design.,* 2009, **9**:633
[12]. Singh S., Gaikwad K.K., Lee M., Lee Y.S. *Journal of Food Measurement and Characterization,* 2018, **12**:588
[13]. Chen M., Li Z., Chen L. *Nano Materials Science,* 2020, **2**:172
[14]. Liu J., Liu K., Feng L., Liu Z., Xu L. *Biomaterials Science,* 2017, **5**:331
[15]. Akhavan O., Ghaderi E. *ACS Nano,* 2010, **4**:5731
[16]. Hu W., Peng C., Luo W., Lv M., Li X., Li D., Huang Q., Fan C. *ACS Nano* 2010, **4**:4317
[17]. Shi L., Chen J., Teng L., Wang L., Zhu G., Liu S., Luo Z., Shi X., Wang Y., Ren L. *Small.,* 2016, **12**:4165
[18]. Yu L., Zhang Y., Zhang B., Liu J. *Scientific Reports.,* 2014, **4**:1
[19]. Azad R., Bezaatpour A., Amiri M., Eskandari H., Nouhi S., Taffa D.H., Wark M., Boukherroub R., Szunerits S. *Applied Organometallic Chemistry,* 2019, **33**:e5059
[20]. Al-Nafiey A., Kumar A., Kumar M., Addad A., Sieber B., Szunerits S., Boukherroub R., Jain S.L. *Journal of Photochemistry and Photobiology A: Chemistry.,* 2017, **336**:198
[21]. Mishra A., Bera G., Mal P., Padmaja G., Sen P., Das P., Chakraborty B., Turpu G. *Applied Surface Science,* 2019, **488**:221
[22]. Zhou X., Zhou M., Ye S., Xu Y., Zhou S., Cai Q., Xie G., Huang L., Zheng L., Li Y. *International Biodeterioration & Biodegradation,* 2021, **162**:105260
[23]. Chen T., Geng Y., Wan H., Xu Y., Zhou Y., Kong X., Wang J., Qi Y., Yao B., Gao Z. *Journal of Alloys and Compounds,* 2021, **876**:160153
[24]. Zhao X., Chen M., Wang H., Xia L., Guo M., Jiang S., Wang Q., Li X., Yang X. *Materials Science and Engineering: C,* 2020, **116**:111221
[25]. Dhandapani P., AlSalhi M.S., Karthick R., Chen F., Devanesan S., Kim W., Rajasekar A., Ahmed M., Aljaafreh M. J. *Journal of Hazardous Materials,* 2021, **409**:124661
[26]. Ansari M.O., Kumar R., Alshahrie A., Abdel-wahab M.S., Sajith V.K., Ansari M.S., Jilani A., Barakat M., Darwesh R. *Composites Part B: Engineering,* 2019, **175**:107092
[27]. Rai B. *Solar cells* 1988, **25**:265
[28]. Adeleye A.S., Oranu E.A., Tao M., Keller A.A. *Water Research,* 2016, **102**:374
[29]. Wan X., Wang J., Zhu L., Tang J. *Journal of Materials Chemistry A.,* 2014, **2**:13641
[30]. Jilani A., Othman M.H.D., Ansari M.O., Oves M., Hussain S.Z., Khan I.U., Abdel-wahab M.S. *Journal of Materials Science,* 2019, **54**:6515
[31]. Huang W.C., Lyu L.M., Yang Y.C., Huang M. H. *Journal of the American Chemical Society,* 2012, **134**:1261
[32]. Perelshtein I., Applerot G., Perkas N., Wehrschuetz-Sigl E., Hasmann A., Gübitz G., Gedanken A. *Surface and Coatings Technology,* 2009, **204**:54
[33]. Lucas J.A., Hawkins N.J., Fraaije B.A. *Advances in Applied Microbiology,* 2015, **90**:29
[34]. Minami T., Nishi Y., Miyata T., Nomoto J.I. *Applied Physics Express,* 2011, **4**:062301
[35]. Ghoreishian S.M., Maleknia L., Mirzapour H., Norouzi M. *Fibers and Polymers,* 2013, **14**:201
[36]. Sunada K., Minoshima M., Hashimoto K. *Journal of Hazardous Materials,* 2012, **235**:265
[37]. Chen L., Tang M., Chen C., Chen M., Luo K., Xu J., Zhou D., Wu F. *Environmental Science & Technology,* 2017, **51**:12663
[38]. Large E. *Annals of Applied Biology,* 1945, **32**:319
[39]. Omae I. *Applied Organometallic Chemistry,* 2003, **17**:81
[40]. Xu Z., Ye S., Zhang G., Li W., Gao C., Shen C., Meng Q. *Journal of Membrane Science,* 2016, **509**:83
[41]. Moghanlou A.O., Bezaatpour A., Sadr M.H., Yosefi M., Salimi F. *Materials Science in Semiconductor Processing,* 2021, **130**:105838
[42]. Huang Y., Xie X., Li M., Xu M., Long J. *Optics Express.,* 2021, **29**:4453

[43]. Song J., Xu L., Zhou C., Xing R., Dai Q., Liu D., Song H. *ACS Applied Materials & Interfaces,* 2013, **5**:12928
[44]. Singh P., Singh K.R., Singh J., Das S.N., Singh R.P. *RSC Advances.,* 2021, **11**:18050
[45]. Kurantowicz N., Sawosz E., Jaworski S., Kutwin M., Strojny B., Wierzbicki M., Szeliga J., Hotowy A., Lipińska L., Koziński R. *Nanoscale research letters.,* 2015, **10**:1
[46]. Gurunathan S., Han J.W., Dayem A.A., Eppakayala V., Kim J.H. *International journal of nanomedicine.,* 2012, **7**:5901
[47]. Diez-Pascual A.M., Diez-Vicente A.L. *ACS applied materials & interfaces.,* 2016, **8**:17902
[48]. Smith A.T., LaChance A.M., Zeng S., Liu B., Sun L. *Nano Materials Science.,* 2019, **1**:31
[49]. Kittler S., Greulich C., Diendorf J., Koller M., Epple M. *Chemistry of materials.,* 2010, **22**:4548
[50]. Kohanski M.A., Dwyer D.J., Hayete B., Lawrence C.A., Collins J.J. *Cell.,* 2007, **130**:797
[51]. Hajipour M.J., Fromm K.M., Ashkarran A.A., de Aberasturi D.J., de Larramendi I.R., Rojo T., Serpooshan V., Parak W.J., Mahmoudi M. *Trends in Biotechnology.,* 2012, **30**:499
[52]. Guzman M., Dille J., Godet S. *Nanomedicine: Nanotechnology, biology and medicine.,* 2012, **8**:37
[53]. Shahverdi A.R., Fakhimi A., Shahverdi H.R., Minaian S. *Nanomedicine: Nanotechnology, Biology and Medicine.,* 2007, **3**:168
[54]. Manke A., Wang L., Rojanasakul Y. *BioMed Research International.,* 2013, 2013. https://doi.org/10.1155/2013/942916.
[55]. Mohanta Y.K., Panda S.K., Bastia A.K., Mohanta T.K. *Frontiers in Microbiology.,* 2017, **8**:626
[56]. Bulcke F., Dringen R. *Neurochemical Research.,* 2015, **40**:15
[57]. Castiglioni S., Caspani C., Cazzaniga A., Maier J.A. *World Journal of Biological Chemistry.,* 2014, **5**:457
[58]. Fahmy B., Cormier S.A. *Toxicology In Vitro.,* 2009, **23**:1365
[59]. Singh N., Turner A. *Environmental Pollution.,* 2009, **157**:371
[60]. Midander K., Cronholm P., Karlsson H.L., Elihn K., Möller L., Leygraf C., Wallinder I.O. *Small.,* 2009, **5**:389
[61]. Karlsson H.L., Cronholm P., Hedberg Y., Tornberg M., De Battice L., Svedhem S., Wallinder I.O. *Toxicology.,* 2013, **313**:59
[62]. VanWinkle B.A., de Mesy Bentley K.L., Malecki J.M., Gunter K.K., Evans I.M., Elder A., Finkelstein J.N., Oberdörster G., Gunter T.E. *Nanotoxicology.,* 2009, **3**:307
[63]. Karlsson H.L., Cronholm P., Gustafsson J., Moller L. *Chemical Research in Toxicology.,* 2008, **21**:1726
[64]. Minocha S., Mumper R.J. *Small.,* 2012, **8**:3289

How to cite this manuscript: Ali Oji Moghanlou*, Farshid Salimi. The Investigation of Antibacterial Activity and Cell Viability of rGO/Cu_2O nanocomposite. *Journal of Medicinal and Nanomaterials Chemistry, 4(1) 2022,* 63-67. DOI: 10.48309/jmnc.2022.1.6